J. Micropalaeontology, 45, 405–413, 2026
https://doi.org/10.5194/jm-45-405-2026

Journal of Micropalaeontology
Open Access

Artificial intelligence applied to the automated detection and identification of Devonian miospores

Vitalina Lokteva[1], Vahram Serobyan[1], Martin Tetard[2], Pierre Breuer[3], and Taniel Danelian[4]

[1]Institute of Geological Sciences of the National Academy of Sciences of the Republic of Armenia, 24A, Marshal Baghramyan Avenue, Yerevan 0019, Republic of Armenia
[2]ESNZ, Lower Hutt, New Zealand
[3]Laboratoire de Paléobotanique, Paléopalynologie et Micropaléontologie, Université de Liège, Allée du 6 août, B18, Sart-Tilman, 4000 Liège, Belgium
[4]Univ. Lille, CNRS, UMR 8198, Evo-Eco-Paleo, 59000 Lille, France

Correspondence: Vahram Serobyan (vahramserobyan@gmail.com)

Received: 11 January 2026 – Revised: 16 April 2026 – Accepted: 30 April 2026 – Published: 19 May 2026

Abstract. Over the last few years, rapid advances in artificial intelligence, especially the application of convolutional neural networks (CNNs), have created new opportunities for automated microscopic image identification. Here we introduce a two-step pipeline for the automated detection and identification of Devonian miospore species by integrating object detection with downstream classification. Our workflow focused on three biostratigraphically important species occurring in the upper Frasnian sedimentary sequences of Armenia: *Teichertospora torquata*, *Geminospora lemurata*, and *Samarisporites triangulatus*. A YOLOv11-based detector localized initially individual miospore specimens on slide images, producing background-free crops and a size measure based on bounding-box area. The detector reached 98 % precision on the test set. The cropped spore images were then classified with the use of three different CNN architectures (VGG16, ResNet-18, and EfficientNet-B0), with size included as an additional numeric feature alongside the image input. Among the three tested models, ResNet-18 performed the best, achieving 87.9 % of classification accuracy. Our results show that combining modern detection with compact classification and morphometric information provides a practical route toward semi-automated palynology for Devonian spores.

1 Introduction

Despite the enormous significance of palynology for numerous applications, miospore studies still rely on time-consuming light microscopy workflows, in which specialists identify and count taxa by examining spore shape, color, symmetry, and ornamentation. Manual identification requires specialized training, scales poorly to large slide collections, and is time-consuming. Recognizing these limitations, efforts to automate taxonomic assessment in palynology began at least 3 decades ago (Stillman and Flenley, 1996). Early attempts to automate the classification process required significant human intervention, which both introduced analyst bias and demanded substantial time for data preparation. Such studies relied on knowledge-based systems (Brough and Alexander, 1986; Beightol and Conrad, 1988; Riedel, 1989) or on hidden Markov model classifiers (García et al., 2012). In contrast, convolutional neural networks (CNNs), first introduced by Fukushima (1980), learn features directly from data and are now actively developed and applied across many microfossil groups (e.g., Beaufort and Dollfus, 2004; Hsiang et al., 2019; Carlsson et al., 2022, 2023; Tetard et al., 2023). During the last decade, CNNs have also been applied to spore and pollen classification (e.g., Sevillano and Aznarte, 2018; Khanzhina et al., 2018; Polling et al., 2021; Olsson et al., 2021; Punyasena et al., 2022; López-García et al., 2023) and detection (Feng et al., 2025). Most studies, however, use images of modern pollen as a training set due to both the availability of the material and its superior quality. When these models are applied to fossil pollen, their accuracy decreases. Bourel et al. (2020) evaluated a multi-CNN

approach on modern, damaged, and fossil pollen assemblages from eastern Africa and reported average per-class misclassification rates of 0.0 % for modern pollen and 2.7 % and 4.1 % for damaged and fossil material, respectively, indicating that performance differs substantially across different states of preservation. Durand et al. (2024) suggested a hierarchical workflow in which six CNNs are integrated under a main CNN. Their approach achieved an average per-class accuracy (APC) of 91 % on recent pollen, whereas performance was lower when applied to fossil pollen images. Fossil spores from the Devonian period have received comparatively little attention.

The aim of the present study is to evaluate the efficacy of deep learning methods for the automated identification of three selected Devonian miospore species, such as *Teichertospora torquata* (Higgs, 1975) McGregor and Playford, 1990; *Samarisporites triangulatus* Allen, 1965; and *Geminospora lemurata* (Balme, 1962) emend. Playford, 1983, which are biostratigraphically significant, widely distributed, and critical for defining global biozones in Gondwana and Laurussia. Indeed, all three index species are particularly useful in biostratigraphic studies integrated in hydrocarbon exploration, especially in Saudi Arabia (Al-Hajri et al., 1999; Breuer, 2007).

2 Materials and methods

The studied material comes from the upper Frasnian succession of the Ertych section in central Armenia (39°43.850′ N, 45°16.300′ E; Fig. 1a). Sampling was carried out during several field campaigns over the last few years. For more details about the lithostratigraphic, biostratigraphic, and chronostratigraphic framework of the studied section, the reader is referred to Serobyan et al. (2023), Khachatryan et al. (2025), Yeghiazaryan et al. (2025), Tsatryan et al. (2025), and Lokteva et al. (2025a). In total, 14 beds were sampled, with miospores recovered from 12 of them (Fig. 1b).

Details about the preparation of the studied samples are given in Khachatryan et al. (2025). Three to five slides were prepared for each productive sample, which were observed afterwards with the use of a Leica DM2700 transmitted-light microscope. All specimens qualitatively identified as *T. torquata* (Fig. 2a), *S. triangulatus* (Fig. 2b), and *G. lemurata* (Fig. 2c) were manually photographed individually with the use of a Flexacam C5 camera.

2.1 Image annotation and datasets

The 209 obtained images were individually annotated by an operator using the web-based software platform Roboflow (Dwyer et al., 2025). Each individual spore was enclosed by a rectangular bounding box. For every annotation, the image ID, class label, and microscope magnification were recorded as metadata. The original microphotographs were annotated to create the base detection dataset. This dataset consisted of five classes: *G. lemurata* (22 %), *S. triangulatus* (19 %), *T. torquata* (16 %), "other" (19 %), and background (24 %), as shown in Fig. 3. Here, the "other" class includes non-target miospore taxa, whereas the background class comprises images without miospores, dominated by phytoclast material.

For training the detection model, the 209 annotated images were split into three different subsets – "train", "validation", and "test" – with a 70/20/10 split. After training, the detection model was applied to the same set of 209 original images to localize spores and export a table linking each source image to its predicted bounding-box area (in pixels) and background-free crops of individual spores. This inference step produced 159 spore crops, which formed the classification dataset. The latter includes four classes (*G. lemurata*, *S. triangulatus*, *T. torquata*, and "other") and was split into three different subsets – "train", "validation", and "test" – with a fixed 70/15/15 split. Alongside each crop, the corresponding bounding-box area was retained as an auxiliary numeric feature for classification.

2.2 Image augmentations

Image augmentation artificially expands the training subset of the original dataset by applying transformations that improve generalization and reduce overfitting. For detection, augmentation was applied before training to the training split of the 209-image annotated detection dataset, using brightness adjustment (-20 % to $+20$ %), random noise (≤ 0.46 % of pixels), horizontal and vertical flips, blur (≤ 1 px), small rotations ($-15°$ to $+15°$), and 90° rotations. The validation and test splits were kept unaugmented. After augmentation, the detection dataset contained 420 training images, 40 validation images, and 20 test images. For classification, augmentation was performed on the fly during training and applied only to the training split of the classification dataset derived from detection. At each training iteration, images were resized to 224×224 pixels and randomly transformed with horizontal and vertical flips, rotations ($\pm 15°$), color jitter, normalization, and random erasing. The classification validation set underwent only resizing, normalization, and tensor conversion, ensuring an unbiased evaluation.

3 Models and metrics

CNNs are tailored to image data by learning local features via stacked convolution, nonlinearity, and pooling. In this study, we used supervised learning, training on labeled images with taxonomic categories as targets. All models were implemented in PyTorch (Paszke et al., 2019) and trained with transfer learning: convolutional feature extractors were frozen, and only task-specific heads for detection and classification were fine-tuned on the miospore data.

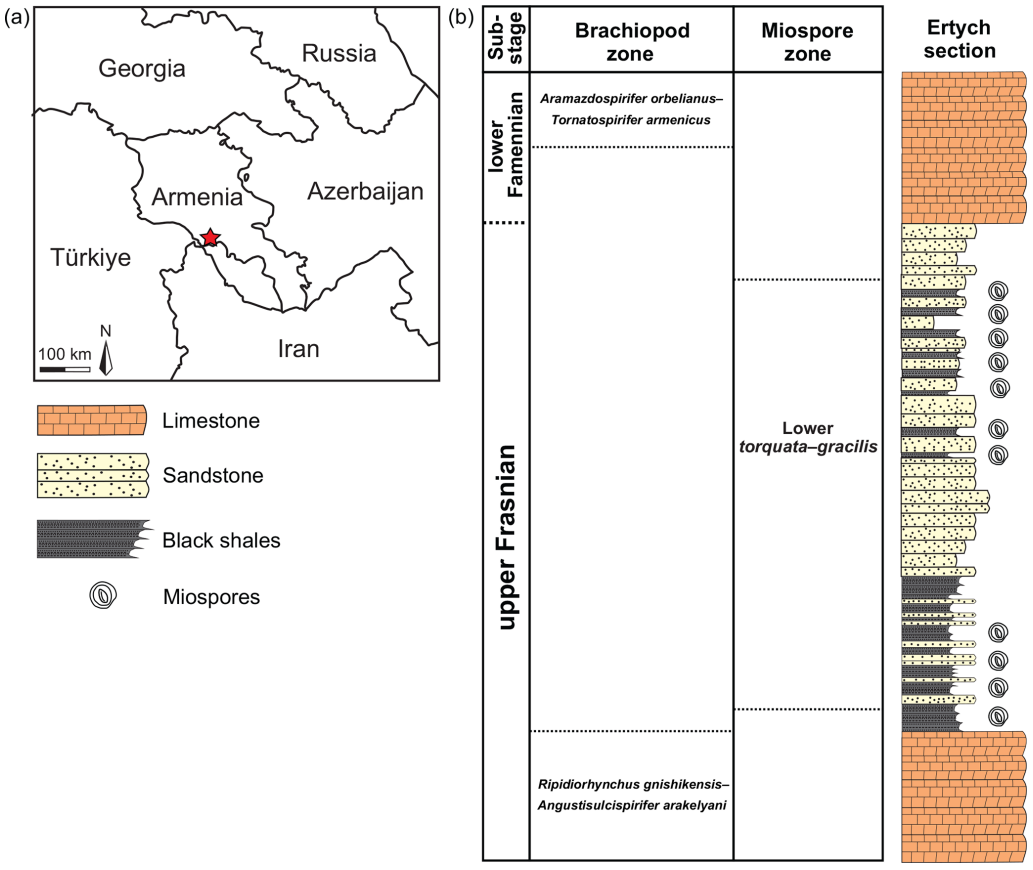

Figure 1. **(a)** Red star indicates the locality of the studied Ertych section in Armenia. **(b)** Stratigraphic framework of the studied material from the upper Frasnian interval of the Ertych section (adapted from Khachatryan et al., 2025).

3.1 Detection model

For detection, YOLOv11, a one-stage network, was used. In a single forward pass, it predicts bounding-box coordinates, objectness, and class probabilities. The model was initialized with COCO-pretrained weights (Redmon et al., 2016). Performance was assessed using precision, recall, and mean average precision (mAP). Precision is defined as the fraction of predicted boxes that are correct, and recall is defined as the fraction of true objects that the model detects. mAP at different intersection-over-union (IoU) thresholds is also reported, where IoU measures the overlap between a predicted and a ground-truth box: mAP@0.5 is computed at a fixed IoU of 0.5, whereas mAP@[0.5 : 0.95] averages mAP over IoU thresholds from 0.5 to 0.95 in steps of 0.05, providing a stricter summary metric of detection quality.

3.2 Classification models

VGG16 (Visual Geometry Group 16) is a 16-layer CNN that stacks small 3×3 convolutions to expand the receptive field while keeping the architecture simple, and it provides a stable, well-understood baseline for image recognition (Simonyan and Zisserman, 2015). ResNet-18 is an 18-layer CNN that employs residual (skip) connections to prevent optimization degradation in deeper models and offers a lightweight, efficient feature extractor (He et al., 2016). EfficientNet-B0 is the baseline model in the EfficientNet family and provides a small footprint suitable for limited data and computes while maintaining strong accuracy (Tan and Le, 2019). Classification performance was assessed using accuracy; macro-F_1 (the mean of per-class F_1 scores, robust in relation to class imbalance); and the Matthew's correlation coefficient (MCC), which condenses the multiclass confusion matrix into a single correlation-like coefficient (ranging from -1 to 1, with 1 denoting perfect, 0 denoting random, and -1 denoting inverted) and is robust in relation to skewed class distributions. In addition, average per-class accuracy (APC), defined as the mean of per-class accuracies, is reported. APC highlights how consistently the model recovers each taxon irrespective of its frequency and therefore complements macro-F_1 and MCC, together providing a clearer picture of performance under the class imbalance typical of palynological datasets.

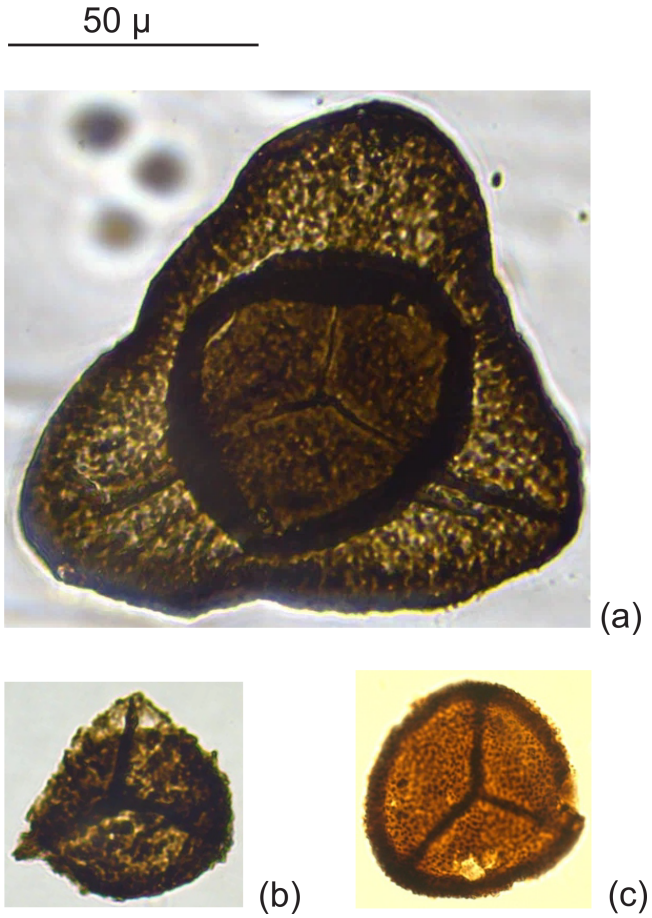

Figure 2. Miospore species from the upper Frasnian deposits of Ertych section, Armenia: **(a)** *Teichertospora torquata* (Higgs, 1975) McGregor and Playford, 1990; **(b)** *Samarisporites triangulatus* Allen, 1965; and **(c)** *Geminospora lemurata* (Balme, 1962) emend. Playford, 1983.

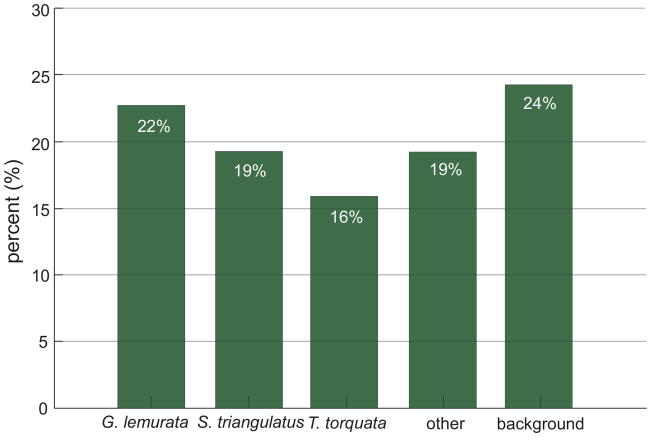

Figure 3. Class distribution in the annotated dataset, based on a total of 209 palynological micrographs containing dispersed miospores.

4 Results

All results reported below were obtained on an independent test set; none of the test images were used for training or validation. This held-out test set, including both images and labels, was used to evaluate the quality of both detection and subsequent classification.

4.1 Detection

The YOLOv11 detector, trained with a single class label "miospore", sequentially processed the test micrographs using a confidence threshold of 0.7. For each detected spore, the bounding-box coordinates (Fig. 4), a cropped image patch, and the crop area (in pixels and calibrated to μm^2) were stored. Precision reached 0.98, recall was 1.0, and mAP@0.5 was 0.995. When averaged across IoU thresholds from 0.5 to 0.95, the model achieved a mean average precision (mAP@[0.5 : 0.95]) of 0.906.

4.2 Classification

The neural networks were trained on a dataset of 159 cropped photographs, augmented with an additional numeric feature in the form of the area of the cropped photograph. We compared three neural networks – EfficientNet-B0, ResNet-18, and VGG16 – in terms of accuracy and other metrics, averaged over 10 runs (Table 1). Regarding the test set, ResNet-18 achieved, on average, the highest accuracy (87.9 %) and MCC (0.85), whereas VGG16 obtained the highest macro-F_1 (87.3 %) with comparable test accuracy (87.5 %). The EfficientNet-B0 model performed below both: the test accuracy was 79.6 %, the test macro-F_1 was 76.4 %, and the test MCC was 0.75. The mean best validation accuracy was also higher for VGG16 (81.2 %) and ResNet-18 (76.2 %) than for EfficientNet-B0 (74.6 %). In the best single runs, the maximum test accuracy reached 95.8 % for ResNet-18 (run 5) and 95.8 % for VGG16 (run 5), EfficientNet's best result was 87.5 % (run 2). Thus, based on average metrics, ResNet-18 leads in terms of accuracy and MCC, VGG16 leads in terms of macro-F_1 with similar accuracy, and EfficientNet-B0 shows lower values for all three metrics. These findings are consistent across both the 10-run averages and the top single-run results and reflect variability across runs.

5 Discussion

This study applied deep learning approaches to the automated detection and identification of Devonian miospores in palynological slides, representing, to our knowledge, a first ever attempt of such. The examined material was recovered from upper Frasnian strata of one of the best-known sections in the region for palynological research. A two-step pipeline combining object detection and supervised taxonomic classification was implemented to rec-

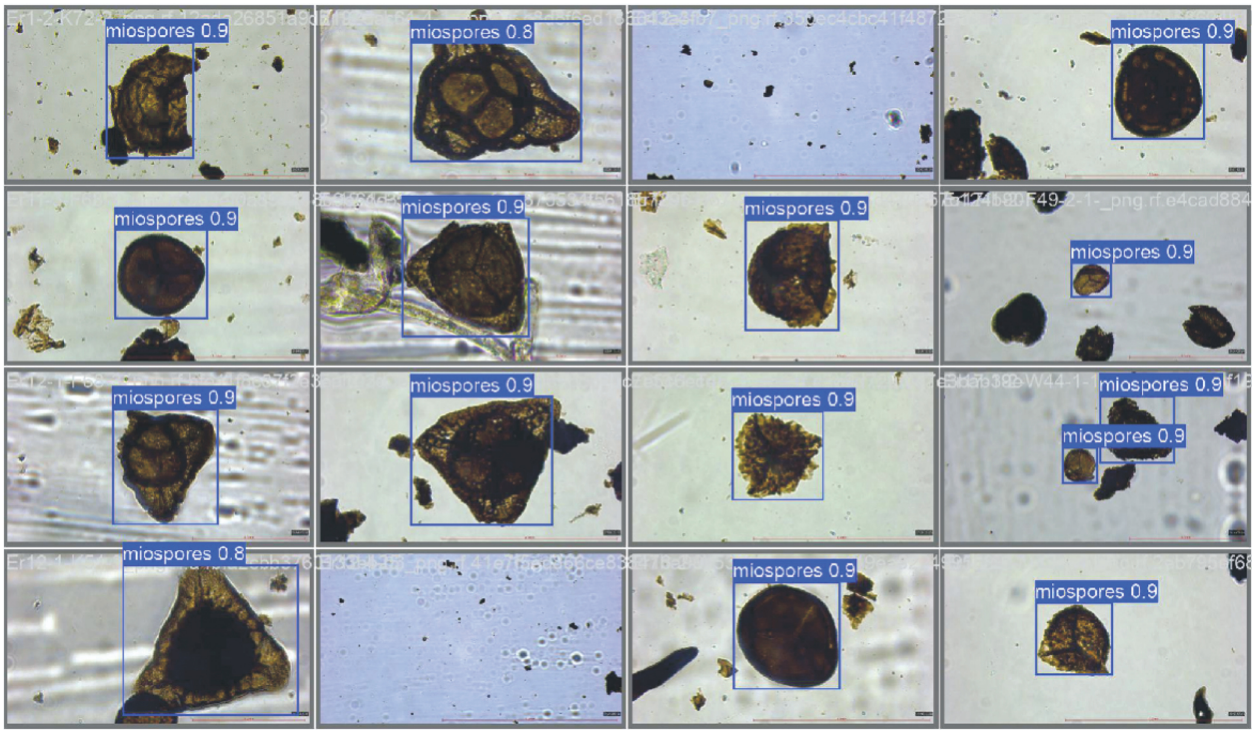

Figure 4. Example results of the YOLOv11 detection model applied to palynological micrographs. Detected miospores are enclosed in blue bounding boxes with corresponding confidence scores.

Table 1. Summary of tests on the images and area size dataset using EfficientNet-B0, ResNet-18, and VGG16. All metrics are means over 10 runs; accuracy and macro-F_1 are reported as percentages, and MCC is unitless.

Architecture	EfficientNet-B0	ResNet-18	VGG16
Inputs	Images + area size		
Number of runs	10		
Epochs per run	30		
Best validation accuracy (mean, %)	74.6	76.2	81.2
Average test accuracy (%) ± SD	79.6 ± 0.10	87.9 ± 0.08	87.5 ± 0.07
Average test macro-F_1 (%) ± SD	76.4 ± 0.13	86.9 ± 0.10	87.3 ± 0.07
Average test MCC ± SD	0.75 ± 0.13	0.85 ± 0.09	0.84 ± 0.08
Average per-class accuracy (%)	86.25	84.5	85.5

ognize three biostratigraphically important species: *Geminospora lemurata*, *Samarisporites triangulatus*, and *Teichertospora torquata*. These miospores are widely applied in Devonian biozonation schemes and, in some regions, constitute key index species in biostratigraphic applications related to oil and gas reservoirs. Accordingly, the proposed workflow has relevance beyond purely academic studies. The two-step pipeline introduced here provides a robust framework for semi-automated palynological analysis, in which individual miospore specimens are first detected and subsequently classified using convolutional neural networks, with bounding-box area being incorporated as an additional feature. During the first step of the pipeline, the YOLOv11-based detector achieved high precision (0.98), recall (1.0), and mAP@0.5 (0.995) on the test set, demonstrating its efficacy in localizing miospores in microscopic images. Automated detection significantly reduces the manual preprocessing required in workflows where images are manually localized and cropped prior to model training (e.g., Gonçalves et al., 2016; Rostami et al., 2025). Because palynological slides typically contain other palynomorphs (e.g., acritarchs, prasinophytes, chitinozoans) and phytoclasts in addition to miospores, this automated detection step streamlines dataset preparation and reduces background interference. Among the three CNN architectures (EfficientNet-B0, ResNet-18, and VGG16) evaluated for classification, ResNet-18 con-

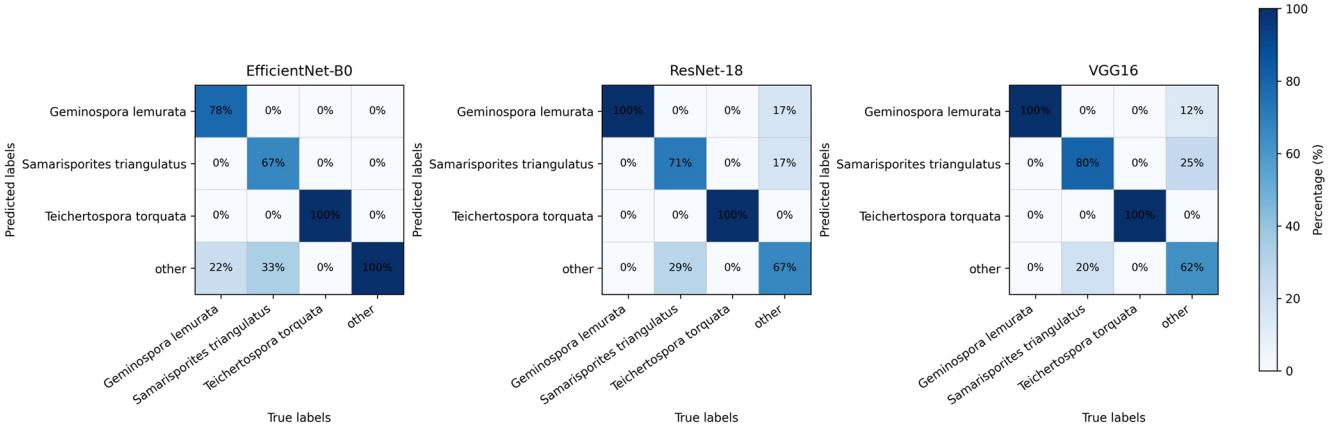

Figure 5. Confusion matrices for EfficientNet-B0, ResNet-18, and VGG16 on the test set. Cells show percentages within each true class; darker shades indicate higher values. Axes: rows – predicted labels; columns – true labels.

sistently achieved the highest mean test accuracy (87.9 %) and Matthews correlation coefficient (MCC = 0.85), indicating strong and balanced performance in discriminating the targeted miospore species (*T. torquata*, *G. lemurata*, and *S. triangulatus*). VGG16 also performed well, yielding the highest mean macro-F_1 score (87.3 %) with comparable test accuracy (87.5 %), whereas EfficientNet-B0 showed lower performance across all metrics (test accuracy of 79.6 %, macro-F_1 of 76.4 %, MCC of 0.75). These performance patterns were consistent across 10-run averages and the best single-run results, indicating methodological robustness. The bounding-box area derived during the detection step proved to be a useful auxiliary feature for classification, particularly where morphological similarity between taxa renders size an important discriminative criterion. However, it is worth noting that model performance varied among species, reflecting differences in morphology and preservation. Per-class F_1 scores, together with the confusion matrix, provide insight into these patterns (Fig. 5). All three classifiers reliably identified *T. torquata*, achieving an F_1 score of 1.00 across all models. This species is characterized by a cavate structure, sub-triangular outline, distinct trilete mark, and relatively large size (Fig. 2a), features that likely facilitate robust recognition by the models. Classification performance was also strong for *G. lemurata*, a cavate miospore with a broadly rounded outline, clear trilete mark, and diameter of approximately 40–50 µm (Fig. 2c), for which per-class F_1 scores ranged between 0.88 and 0.92. In contrast, performance was lower for *S. triangulatus*, which exhibits a rounded-triangular outline, an indistinct trilete mark, cone-shaped sculpture, and a size of about 45–60 µm (Fig. 2b); F_1 scores for this species ranged from 0.73 to 0.80. This reduced performance likely reflects the poorer state of preservation of *S. triangulatus* in the available material, which obscures diagnostic features, whereas the larger size and more distinctive morphology of *T. torquata* (up to 85–140 µm) enhance model reliability.

In addition to the classes represented, classification accuracy is also influenced by dataset characteristics and the evaluation protocol. The dataset was comprised of 159 microphotographs prior to augmentation, which, although sufficient for a proof-of-concept study, inevitably introduces variance in performance estimates. The inclusion of a heterogeneous "other" class, aggregating diverse taxa, further increases within-class variability. Moreover, all images were acquired using a single microscope and a single preparation protocol; therefore results may vary when the method is applied to material prepared or imaged under different conditions. Despite these limitations, the pipeline produced consistent and satisfactory results, with a detection mAP@0.5 of 0.995 and classification average per-class accuracies of 84.5 %–86.25 %. These values fall within the range reported in recent palynological and microfossil classification studies (approximately 83.3 %–99.8 %; Sevillano and Aznarte, 2018; Khanzhina et al., 2018; Bourel et al., 2020; Polling et al., 2021; Punyasena et al., 2022; Durand et al., 2024), highlighting the comparability of the present results despite differences in taxa, image quality, and dataset size.

The approach could be further extended by enlarging the image dataset, broadening the taxonomic coverage, incorporating material from additional sections and laboratories, and integrating the detector with automated slide-scanning systems to increase analytical throughput. It is important to emphasize that supervised AI-based classification remains dependent on expert-defined taxonomic concepts and carefully curated training datasets. Rather than replacing specialist knowledge, the proposed workflow functions as a screening and decision support tool that helps standardize routine identification tasks, reduce observer bias, and improve reproducibility. By accelerating the detection of index species and enabling rapid screening of large image datasets, this approach facilitates more efficient taxonomic assessment, biostratigraphic analysis, and stratigraphic interpretation.

6 Conclusions

This study demonstrates that deep learning-based methods can be effectively applied to the automated detection and identification of biostratigraphically important Devonian miospores in palynological slides. A two-step workflow combining object detection and convolutional neural network-based classification achieved high detection accuracy, with the YOLOv11 model providing reliable localization of palynomorphs even in complex backgrounds affected by preservation and matrix variability. Furthermore, convolutional neural networks (VGG16, ResNet-18, and EfficientNet-B0) trained on labeled palynological slides provided robust classification performance, with ResNet-18 achieving the highest accuracy of up to 87.9 %. The integration of simple morphometric information, such as bounding-box area, enhanced taxonomic discrimination and proved to be particularly valuable for larger and morphologically distinctive taxa. Taken together, the results show that combining image-based pattern recognition with quantitative size information yields a scalable, reproducible, and efficient workflow suitable for routine palynological analysis. While further improvements will require larger, more diverse training datasets and broader taxonomic coverage, the proposed approach provides a solid methodological foundation for semi-automated biostratigraphic studies and offers potential for future extension to other fossil groups, including Paleozoic marine phytoplankton such as acritarchs and prasinophytes, as well as scolecodonts.

Code availability. The code is available at Zenodo: https://doi.org/10.5281/zenodo.18032045 (Lokteva et al., 2025b).

Data availability. The annotated dataset in YOLOv11 PyTorch format, along with the associated metadata, was uploaded to Zenodo: https://doi.org/10.5281/zenodo.18032045 (Lokteva et al., 2025b).

Sample availability. All analyzed slides are stored at the Institute of Geological Sciences, National Academy of Sciences of Armenia (Yerevan), and the remaining shale samples are curated by the paleontology team at the University of Lille (France).

Author contributions. VL and VS designed the study. VL was responsible for the writing (original draft and editing). VL collected and processed the microscopy images, carried out model development, and analyzed the data. VL and PB did the taxonomic identification. VS and TD contributed with resources and material. VS, TD, and MT supervised the work.

Competing interests. At least one of the (co-)authors is a member of the editorial board of *Journal of Micropalaeontology*. The peer-review process was guided by an independent editor, and the authors also have no other competing interests to declare.

Disclaimer. Publisher's note: Copernicus Publications remains neutral with regard to jurisdictional claims made in the text, published maps, institutional affiliations, or any other geographical representation in this paper. The authors bear the ultimate responsibility for providing appropriate place names. Views expressed in the text are those of the authors and do not necessarily reflect the views of the publisher.

Acknowledgements. The fieldwork was facilitated by the logistic support of the Institute of Geological Sciences (National Academy of Sciences of the Republic of Armenia). Sylvie Regnier from the University of Lille is gratefully acknowledged for preparing the palynological slides. The paper benefited from the constructive reviews of John Marshall and an anonymous reviewer, to whom we are sincerely grateful.

Financial support. The research was supported by the Higher Education and Science Committee of the Ministry of Education, Science, Culture, and Sports of the Republic of Armenia (Research project no. 22RL 016).

Review statement. This paper was edited by Luke Mander and reviewed by John Marshall and one anonymous referee.

References

Al-Hajri, S. A., Filatoff, J., Wender, L. E., and Norton, A. K.: Stratigraphy and operational palynology, GeoArabia, 4, 53–68, https://doi.org/10.2113/geoarabia040153, 1999.

Allen, K. C.: Lower and Middle Devonian spores of north and central Vestspitsbergen, Palaeontology, 8, 687–748, 1965.

Balme, B.: Upper Devonian (Frasnian) spores from the Carnarvon Basin, Western Australia, PaIaeobotanist, 9, 1–10, https://doi.org/10.54991/jop.1960.590, 1962.

Beaufort, L. and Dollfus, D.: Automatic recognition of coccoliths by dynamical neural networks, Mar. Micropaleontol., 51, 57–73, https://doi.org/10.1016/j.marmicro.2003.09.003, 2004.

Beightol, D. S. and Conrad, M. A.: Expert systems identify fossils and manage large paleontological databases, Geobyte, 3, 42–46, 1988.

Bourel, B., Marchant, R., de Garidel-Thoron, T., Tetard, M., Barboni, D., Gally, Y., and Beaufort, L.: Automated recognition by multiple convolutional neural networks of modern, fossil, intact and damaged pollen grains, Comput. Geosci., 140, 104498, https://doi.org/10.1016/j.cageo.2020.104498, 2020.

Breuer, P.: Devonian miospore palynology in Western Gondwana: an application to oil exploration, Ph.D. thesis, Université de Liège, Belgium, 115 pp., Volume I: Explanatory notes, 2007.

Brough, D. R. and Alexander, I. F.: The fossil expert system, Expert Syst., 3, 76–83, https://doi.org/10.1111/j.1468-0394.1986.tb00197.x, 1986.

Carlsson, V., Danelian, T., Boulet, P., Devienne, P., Laforge, A., and Renaudie, J.: Artificial intelligence applied to the classification of eight middle Eocene species of the genus *Podocyrtis* (polycystine radiolaria), J. Micropalaeontol., 41, 165–182, https://doi.org/10.5194/jm-41-165-2022, 2022.

Carlsson, V., Danelian, T., Tetard, M., Meunier, M., Boulet, P. Devienne, P., and Ventalon, S.: Convolutional neural network application on a new middle Eocene radiolarian dataset, Mar. Micropaleontol., 183, 102268, https://doi.org/10.1016/j.marmicro.2023.102268, 2023.

Durand, M., Paillard, J., Ménard, M-P., Suranyi, T., Grondin, P., and Blarquez, O.: Pollen identification through convolutional neural networks: First application on a full fossil pollen sequence, PLoS ONE, 19, e0302424, https://doi.org/10.1371/journal.pone.0302424, 2024.

Dwyer, B., Nelson, J., and Hansen, T.: Roboflow (Version 1.0), https://roboflow.com (last access: 7 January 2026), 2025.

Feng, J. T., Puthanveetil, S., Kong, S., Donders, T. H., and Punyasena, S. W.: Addressing the "open world": detecting and segmenting pollen on palynological slides with deep learning, Paleobiology, 51, 394–407, https://doi.org/10.1017/pab.2025.10059, 2025.

Fukushima, K.: Neocognitron: A self-organizing neural network model for a mechanism of pattern recognition unaffected by shift in position, Biol. Cybern., 36, 193–202, https://doi.org/10.1007/BF00344251, 1980.

García, N. M., Chaves, V. A. E., Briceno, J. C., and Travieso, C. M.: Pollen grains contour analysis on verification approach, in: Proceedings of the 7th international conference, Hybrid Artificial Intelligent Systems, Salamanca, Spain, 28–30 March 2012, 521–532, https://doi.org/10.1007/978-3-642-28942-2_47, 2012.

Gonçalves, A. B., Souza, J. S., Silva, G. Gd., Cereda, M. P., Pott, A., Naka, M. H., and Pistori, H.: Feature Extraction and Machine Learning for the Classification of Brazilian Savannah Pollen Grains, PLoS ONE, 11, e0157044, https://doi.org/10.1371/journal.pone.0157044, 2016.

He, K., Zhang, X., Ren, S., and Sun, J.: Deep residual learning for image recognition, in: Conference Proceedings, IEEE Conference on Computer Vision and Pattern Recognition, Las Vegas, NV, USA, 27–30 June 2016, 770–778, https://doi.org/10.48550/arXiv.1512.03385, 2016.

Higgs, K.: Upper Devonian and Lower Carboniferous miospore assemblages from Hook Head, County Wexford, Ireland, Micropaleontol., 21, 393–419, https://doi.org/10.2307/1485291, 1975.

Hsiang, A. Y., Brombacher, A., Rillo, M. C., Mleneck-Vautravers, M. J., Conn, S., Lordsmith, S., Jentzen, A., J. Henehan, M., Metcalfe, B., Fenton, I. S., Wade, B. S., Fox, L., Meilland, J., Davis, C. V., Baranowski, U., Groeneveld, J., Edgar, K. M., Movellan, A., Aze, T., Dowsett, H. J., Miller, C. G., Rios, N., and Hull, P. M.: Endless Forams: > 34,000 modern planktonic foraminiferal images for taxonomic training and automated species recognition using convolutional neural networks,Paleoceanogr. Paleoclimatol., 34, 1157–1177, https://doi.org/10.1029/2019PA003612, 2019.

Khachatryan, S., Cascales-Minana, B., Danelian T., Breuer, P., Steemans, P., Grigoryan, A., Gabrielyan, I., Hairapetian, V., Regnier, S., Kroeck D. M., and Serobyan, V.: First palynological evidence from the Upper Devonian of Armenia (northern Gondwanan margin): biostratigraphic implications, Palaeoworld, 34, 100879, https://doi.org/10.1016/j.palwor.2024.09.003, 2025.

Khanzhina, N., Putin, E., Filchenkov, A., and Zamyatina, E.: Pollen grain recognition using convolutional neural network, in: ESANN 2018 Proceedings, European Symposium on Artificial Neural Networks, Computational Intelligence and Machine Learning, Bruges, Belgium, 25–27 April 2018, 409–414, ISBN 978-287587047-6, 2018.

Lokteva, V., Kirakosyan, G., Camina, S. C., De Backer, T., Grigoryan, A., Danelian, T., and Serobyan, V.: Chitinozoans from the upper Frasnian (Upper Devonian) of Armenia: biostratigraphical and palaeobiogeographical implications, Palynology, 2537704, https://doi.org/10.1080/01916122.2025.2537704, 2025a.

Lokteva, V., Serobyan, V., Tetard, M., Breuer, P., and Danelian, T.: Artificial Intelligence applied to the automatic detection and identification of three Devonian miospores, Zenodo [code and data set], https://doi.org/10.5281/zenodo.18032045, 2025b.

López-García, F., Valiente-González, J. M., Escriche-Roberto, M. I., Juan-Borras, M. D. S., Viaquert-Fas, M., Atienza, V., and Agustí-Melchor, M.: Classification of Honey Pollens with ImageNet Neural Networks, in: Proceedings of the 20th International Conference, Computer Analysis of Images and Patterns, Limassol, Cyprus, 25–28 September 2023, 192–200, https://doi.org/10.1007/978-3-031-44240-7_19, 2023.

McGregor, D. C. and Playford, G.: Morphology and distribution of the miospore *Teichertospora torquata* comb. nov. in the Upper Devonian of Euramerica and Australia, Palynology, 14, 7–18, https://doi.org/10.1080/01916122.1990.9989368, 1990.

Olsson, O., Karlsson, M., Persson, A. S., Smith, H. G., Varadarajan, V., Yourstone, J., and Stjernman, M.: Efficient, automated and robust pollen analysis using deep learning, Methods Ecol. Evol., 12, 850–862, https://doi.org/10.1111/2041-210X.13575, 2021.

Paszke, A., Gross, S., Massa, F., Lerer, A., Bradbury, J., Chanan, G., Killeen, T., Lin, Z., Gimelshein, N., Antiga, L., Desmaison, A., Köpf, A., Yang, E., DeVito, Z., Raison, M., Tejani, A., Chilamkurthy, S., Steiner, B., Fang, L., Bai, J., and Chintala, S.: PyTorch: An Imperative Style, High-Performance Deep Learning Library, in: Proceedings of the 33rd International Conference, Neural Information Processing System, Vancouver, Canada, 8–14 December 2019, 8026–8037, https://doi.org/10.48550/arXiv.1912.01703, 2019.

Playford, G.: The Devonian miospore genus *Geminospora* Balme 1962: a reappraisal based upon topotypic *G. lemurata* (type species), Mem. Assoc. Australas. Palaeontol., 1, 311–325, 1983.

Polling, M., Li, C., Cao, L., Verbeek, F., de Weger, L. A., Belmonte, J., De Linares, C., Willemse, J., de Boer, H., and Gravendeel, B.: Neural networks for increased accuracy of allergenic pollen monitoring, Sci. Rep., 11, 11357, https://doi.org/10.1038/s41598-021-90433-x, 2021.

Punyasena, S. W., Haselhoest, D. S., Kong, S., Fowlkes, C. C., and Moreno, J. E.: Automated identification of diverse Neotropical pollen samples using convolutional neural networks, Methods Ecol. Evol., 13, 2049–2064, https://doi.org/10.1111/2041-210X.13917, 2022.

Redmon, J., Divvala, S., Girshick, R., and Farhadi, A.: You only look once: Unified, real-time object detection, in: Conference

Proceedings, IEEE Conference on Computer Vision and Pattern Recognition, Las Vegas, NV, USA, 27–30 June 2016, 779–788, https://doi.org/10.48550/arXiv.1506.02640, 2016.

Riedel, W. R.: Identify: a Prolog program to help identify fossils, Comput. Geosci., 15, 809–823, https://doi.org/10.1016/0098-3004(89)90083-6, 1989.

Rostami, M. A., Kydd, L., Balmaki, B., Dyer, L. A., and Allen, J. M.: Deep learning for accurate classification of conifer pollen grains: enhancing species identification in palynology, Front. Big Data, 14, 1507036, https://doi.org/10.3389/fdata.2025.1507036, 2025.

Serobyan, V., Danelian, T., Hairapetian, V., Crônier, C., Grigoryan, A., Randon, C., and Mottequin, B.: Frasnian (Upper Devonian) brachiopods from Armenia: biostratigraphic and palaeobiogeographic implications, Riv. Ital. Paleontol. S., 129, 373–409, https://doi.org/10.54103/2039-4942/19826, 2023.

Sevillano, V. and Aznarte, J. L.: Improving classification of pollen grain images of the POLEN23E dataset through three different applications of deep learning convolutional neural networks, PloS ONE, 13, e0201807, https://doi.org/10.1371/journal.pone.0201807, 2018.

Simonyan, K. and Zisserman, A.: Very Deep Convolutional Networks for Large-Scale Image Recognition, SSRN Electron. J., 12, 301–307, https://doi.org/10.48550/arXiv.1409.1556, 2015.

Stillman, E. C. and Flenley, J. R.: The needs and prospects for automation in palynology, Quaternary Sci. Rev., 15, 1–5, https://doi.org/10.1016/0277-3791(95)00076-3, 1996.

Tan, M. and Le, Q.: Efficientnet: Rethinking model scaling for convolutional neural networks, in: ICML, 36th International Conference on Machine Learning, Long Beach, CA, USA, 10–15 June 2019, 6105–6114, https://doi.org/10.48550/arXiv.1905.11946, 2019.

Tetard, M., Carlsson, V., Meunier, M., and Danelian, T.: Merging databases for CNN image recognition, increasing bias or improving results?, Mar. Micropaleontol., 185, 102296, https://doi.org/10.1016/j.marmicro.2023.102296, 2023.

Tsatryan, M., Serobyan, V., Grigoryan, A., Avagyan, N., Danelian, T., and Hairapetian, V.: Upper Frasnian conodont biostratigraphy of the Noravank section (Central Armenia), Rev. Micropaléontol., 88, 100845, https://doi.org/10.1016/j.revmic.2025.100845, 2025.

Yeghiazaryan, M., Kroeck, D. M., Danelian, T., Grigoryan, A., Regnier, S., and Serobyan, V.: Acritarchs and prasinophytes from the Upper Devonian of Armenia: biostratigraphical and palaeobiogeographical implications, Palynology, 49, 2445040, https://doi.org/10.1080/01916122.2024.2445040, 2025.